Emissions and performance tradeoffs for advanced marine diesel propulsion

Author(s):
Stefanopoulou, Anna; Smith, Roy

Publication date:
1998-10

Permanent link:
https://doi.org/10.3929/ethz-b-000540169

Originally published in:
IFAC Proceedings Volumes 31(30), https://doi.org/10.1016/S1474-6670(17)38414-8

Emissions and Performance Tradeoffs for Advanced Marine Diesel Propulsion

Anna Stefanopoulou[†] and Roy Smith[‡]

[†]Dept. of Mechanical & Environmental Engineering
[‡]Dept. of Electrical & Computer Engineering,
University of California, Santa Barbara, CA 93106

Abstract: A multivariable control scheme is designed that reduces smoke generation on an experimental marine Diesel engine equipped with a variable geometry turbocharger (v). The variable geometry turbocharger allows the improvement of the steady-state ship hydrodynamic and propulsion characteristics and requires coordination with the injected mass fuel to achieve a good transient performance. *Copyright ©1998 IFAC*

Keywords: Marine propulsion; Multivariable control; Emissions;

1 Introduction

Currently many international ports consider imposing stringent emissions requirements in offshore vehicles. In view of these new requirements, the shipping industry must develop technology to control emissions during ship transient maneuvers. Although, various innovative propulsion configurations which are not based on the IC engine [10] attempt to achieve this goal, the advantages of turbocharged diesel engines render them common practice for the vast majority of ocean freighters and offshore vehicles. In marine propulsion, the turbocharger, the engine, and the propeller operation is optimized to achieve the rated power and maximum torque output. Thus, the turbocharger size is determined for high torque output which usually leads to large effective flow area and consequently slow response. A mechanism that can potentially mitigate the inherent performance tradeoff between maximum power and transient torque response is the variable geometry turbocharger. A turbine with variable geometry uses inlet guide vanes (v) on the turbine stator to modify its effective flow area as shown in Figure 1. Changing the effective turbine flow area is advantageous. First, it provides a better match between the turbocharger and the diesel engine in steady-state [5]. Secondly, it modifies the power transfer to the turbine and, hence, to the compressor which can potentially reduce the turbolag by speeding up the turbocharger response [7, 8].

In this paper we assess the feasibility and potential benefits of variable geometry turbocharger diesel engine for transient ship maneuvers and emission control. Several studies in automotive applications (see [3, 6] for passenger vehicles and [7, 8] for heavy commercial vehicles) have shown promising results. The intent here is to coordinate the injected fuel (W_f) and the variable geometry turbocharger (v) to jointly manage the fuel/air mixture into the cylinders. The multi-input multi-output (MIMO) controller is shown to improve torque and emission generation in marine diesel propulsion.

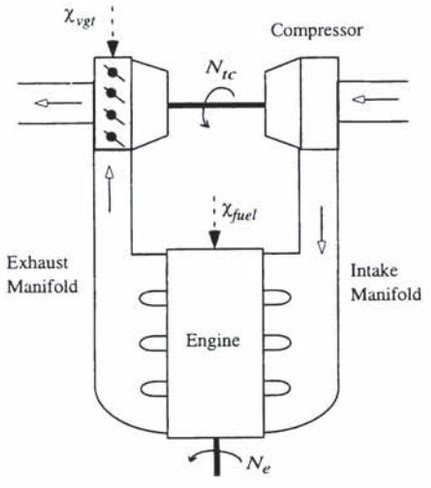

Figure 1: Schematic representation of the VGT diesel engine.

In comparison to the MIMO controller we consider the conventional diesel engine governor. Such a governor controls the combustion fuel supply during changes in load to maintain constant engine speed,

[†] Corresponding author, phone: (805) 893–8501, e-mail: anna@engineering.ucsb.edu. Research supported in part by the NSF under contract ECS-97-33293; matching funds were provided by Turbodyne Inc.

[‡]R. Smith supported by NSF under contract ECS–9634498.

and consequently, constant heading speed. A comprehensive review of mechanical and electronic fuel governors can be found in [4] and [1]. The actual injected fuel is restricted by the injection delays [9] and limiters that are employed to protect the shaft and prevent smoke. Smoke is generated during fast fueling transients by rich air-to-fuel ratio mixtures. Part of the energy in the combusted fuel is stored in the exhaust gas which is used by the turbocharger to spin up to a new steady-state operating point and eventually increase the amount of air to the engine. Thus, changes in fueling rate cause a disturbance in air-to-fuel ratio (ϕ) which is partially rejected through the natural feedback that the turbocharger establishes between the engine exhaust and intake processes. It takes, however, a certain amount of time for the turbocharger to spin up and for the intake manifold to fill to a new level of pressure and air mass, thus, reaching a new equilibrium. The slow dynamics in the engine air flow path causes a drop in the ϕ level which is associated to high hydrocarbon emissions and visible smoke generation. Any further drop in the ϕ level below the stoichiometric value affects the torque output as described in [9].

The variable geometry turbocharger provides an extra degree of freedom to (i) to speed up the air loop dynamics, and consequently, reduce smoke generation without compromising the engine torque response and (ii) to improve steady-state ship speed. The controller must achieve satisfactory tradeoffs between conflicting goals such as maneuverability, fuel economy and emissions. Designing a model based controller requires a low order and accurate representation of the engine and the propeller/surge dynamics. Section 3 describes the model for the turbocharger, engine, and surge dynamics. The steady-state optimization and plant linearization are presented in Section 4 and Section 5. The control design and simulation results with projection on emissions benefits are included in Section 6 and Section 7.

2 Nomenclature

The variables used in this paper are defined below. Other plant constants used in the mathematical model will be described in the text.

Variables		Super/Sub-scripts	
m,	mass (kg)	1,	intake manifold
W,	flow rate (kg/sec)	2,	exhaust manifold
V,	volume (m^3)	f,	fuel
T,	temperature (K)	c,	compressor
Q,	torque (Nm)	t,	turbine
N,	rot. speed (rpm)	o,	ambient
P	power, (W)	e,	engine
Ψ	force (N)	p,	propeller
u	velocity (knots)	r,	resistance

3 Plant Model

The variable geometry turbocharged diesel engine is described briefly with the following equations. The intake and exhaust manifolds are represented as finite volumes based on the "Filling and Emptying Methods" of plenum modeling described in [2]. The dynamic equations that characterize the manifold filling dynamics (Eq. 3.1-3.4) are based on the principles of conservation of mass, conservation of energy, and the ideal gas law.

Intake Manifold

$$\frac{d}{dt}m_1 = W_c - W_e, \tag{3.1}$$

$$\frac{d}{dt}p_1 = \frac{\gamma R}{V_1}\left(W_c T_o - W_e T_1\right), \tag{3.2}$$

Exhaust Manifold

$$\frac{d}{dt}m_2 = W_e + W_f - W_t, \tag{3.3}$$

$$\frac{d}{dt}p_2 = \frac{\gamma R}{V_2}\left((W_e + W_f)T_e - W_t T_2\right), \tag{3.4}$$

In the above, $R = c_p - c_v$ and $\gamma = \frac{c_p}{c_v}$. For simplicity, the same values of specific heats at constant pressure, c_p, and volume, c_v, are used for both intake and exhaust manifolds. In the above equations the heat transfer in the walls is neglected. This assumption is accurate for the intake manifold but it may not hold for the exhaust manifold due to the high exhaust temperature. The air into the intake manifold is assumed to be homogeneous. In addition to the above equations, the principle of conservation of momentum is also satisfied by assuming uniform pressure and temperature between the manifold restrictions.

The right-hand side of the above equations are determined using the engine and turbocharger manufacturer data. In particular, engine manufacturer data is used to describe (i) the engine volumetric efficiency, and consequently, the engine mass air flow rate, W_e, (ii) the temperature rise between the engine intake and exhaust process, $T_e - T_1$, and (iii) the engine brake torque, Q_e that is used in Eq. 3.6 below.

Acceleration of the turbocharger (Eq. 3.5) and engine (Eq. 3.6)is derived using Newton's Second Law.

Rotational Dynamics

$$\frac{d}{dt}N_{tc} = \frac{P_t - P_c}{I_{tc}N_{tc}}, \tag{3.5}$$

$$\frac{d}{dt}N_e = \frac{Q_e - Q_p}{I_e + I_{add}}, \tag{3.6}$$

In the above, I_{tc} and $I_e + I_{add}$ are the mass polar moment of inertia of the rotating systems. The turbine power and the compressor power, P_t and P_c respectively, are calculated based on an ideal adiabatic process, and steady-state data provided by the turbocharger manufacturer. In particular, a "turbine map", f_t, is used to determine the pressure ratio between the upstream and the downstream turbine pressures, $\frac{p_o}{p_2}$, and the efficiency, η_t, based on the turbine flow, W_t, the turbocharger speed, N_{tc}, and the inlet guide vanes position, v.

$$\begin{bmatrix} \frac{p_o}{p_2} \\ \eta_t \end{bmatrix} = f_t\left(W_t, N_{tc}, v\right), \tag{3.7}$$

$$P_t = W_t c_p \eta_t \eta_m T_2 \left(1 - (\frac{p_o}{p_2})^{(\frac{\gamma-1}{\gamma})}\right) \tag{3.8}$$

Similarly, using data from the "compressor map" we can obtain the compressor characteristics.

$$\begin{bmatrix} \frac{p_1}{p_o} \\ \eta_c \end{bmatrix} = f_c\left(W_c, N_{tc}\right), \tag{3.9}$$

$$P_c = W_c c_p \frac{1}{\eta_c} T_o \left((\frac{p_1}{p_o})^{(\frac{\gamma-1}{\gamma})} - 1\right) \tag{3.10}$$

Finally, the propeller torque, Q_p in Eq. 3.6, depends on the ship speed which is calculated based on Newton's First Law.

Surge Dynamics

$$\frac{d}{dt}u = \frac{\Psi_p - \Psi_r}{m_\nabla + m_{hydro}}, \tag{3.11}$$

The ship displacement and the hull wetted surface added virtual mass are denoted by $m_\nabla + m_{hydro}$ in the equation above. The propeller torque, Q_p, and thrust, Ψ_p, are determined using open water cavitation tank data supplied by the manufacturer, k_Q and k_Ψ respectively, and are modified by hydrodynamic interactions between hull and propeller:

$$Q_p = \rho N_p^2 D_p^5 k_Q(J), \tag{3.12}$$

$$\Psi_p = (1-t)\rho N_p^2 D_p^4 k_\Psi(J), \tag{3.13}$$

$$J = \frac{u(1-w)}{N_p D_p}, \tag{3.14}$$

where, w and t are the wake fraction and thrust deduction (assumed to be constant), and k_Q and k_ψ are the wake and thrust coefficients (approximated by linear polynomials in the advance coefficient, J). The propeller speed, $N_p = N_e/gr$, is determined assuming a fixed gear ratio, and D_p is the propeller diameter.

The actuator dynamics are modeled as first order differential equations. The break frequency is defined by the stable and closed inner loop hydraulic controller.

Actuator Dynamics

$$\frac{d}{dt}W_f = \frac{1}{\tau_f}\left(\chi_{fuel} - W_f\right), \tag{3.15}$$

$$\frac{d}{dt}v = \frac{1}{\tau_v}\left(\chi_{vgt} - v\right), \tag{3.16}$$

The actuation signals, χ_{fuel} and χ_{vgt}, are generated by the control system, and the time constants, τ_f and τ_v, are approximately equal to 0.1 sec.

Equation 3.1-3.6, 3.11, and 3.15-3.16 constitute the nine states of the dynamic plant model, $[m_1, p_1, m_2, p_2, N_{tc}, N_e, u, W_f, v]$.

4 Steady-State Optimization

The ship operator command usually involves a desired maneuver such as a sudden acceleration/deceleration or maintaining constant ship speed during wave induced disturbances. The controller is designed to meet this operator command, while satisfying constraints in emissions and fuel economy. This objective imposes both steady-state and transient requirements. We analyze the steady-state requirements of the control design goals by studying the equilibrium points of the dynamic model discussed above. The model is simulated for a range of fueling levels, χ_{fuel}, and inlet guide vane positions, χ_{vgt}, and the achieved equilibriums are tabulated. We note here that for each pair of $(\chi_{fuel}, \chi_{vgt})$ values we obtain a unique equilibrium which is asymptotically stable. Figure 2 shows the steady-state ship speed, u, engine speed, N_e, and air-to-fuel ratio, ϕ, plotted versus χ_{vgt} for different values of χ_{fuel}.

Firstly, for efficient marine propulsion it is desired to choose an inlet guide vane position that maximizes ship speed for a given constant fueling level. The χ_{vgt} values that achieve the maximum ship speed objective for each fueling level, from 5 kg/hr to 13 kg/hr, are shown with the dotted line in the upper subplot of Figure 2. It is evident from the N_e-subplot of Figure 2 that the steady-state engine speed and the steady-state ship speed are maximized for the same χ_{vgt} values.

Secondly, the emission constraints that we consider in this paper are related to smoke generation, and more generally, to hydrocarbon (HC) and particulate emissions. Large air-to-fuel ratios, ϕ, correlate with low hydrocarbon (HC) and particulate emissions. Hence, to reduce these type of emissions it is desired to choose χ_{vgt} that results in high air-to-fuel ratio, and in particular, an air-to-fuel ratio greater than 24 (limit for visible smoke generation). The χ_{vgt} values that achieve the maximum ϕ for each fueling

level from 5 kg/hr to 13 kg/hr are connected with the dot-dash line in the lower subplot of Figure 2.

Obviously the "maximum u" and "maximum ϕ" objectives cannot be satisfied simultaneously and the solid line (denoted by "selected setpoints" in Figure 2) represents the χ^*_{vgt} values for which the best tradeoff between fuel economy and emissions is achieved for each fueling level. The "selected setpoints" line is also shown on the N_e-subplot in Figure 2.

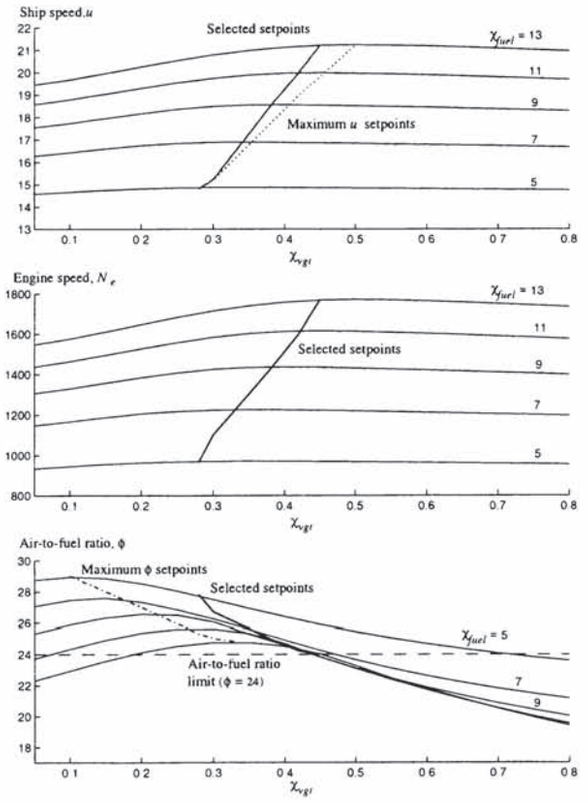

Figure 2: Steady-state ship speed, u, engine speed, N_e, and air-to-fuel ratio, ϕ.

Using the above selected data and polynomial interpolation , a feedforward controller that calculates the desired steady-state engine speed, N_e^*, and air-to-fuel ratio, ϕ^*, based on the ship speed command, u^*, is derived. In Section 6 a linear multivariable feedback controller is designed that ensures tracking of the desired setpoints.

5 Dynamic Open Loop Characteristics

The frequency domain characteristics of the linearized plant are presented to better understand the interactions between the performance variables, N_e and ϕ, and the actuators, χ_{fuel} and χ_{vgt}. Linearization is performed at a nominal point, $\chi^*_{fuel} = 9.0$ kg/hr, and $\chi^*_{vgt} = 0.38$. Bode magnitude plots in Figure 3 describe the dynamic relation between the output scaled variables, $N_e/2000$ and $\phi/10$, and the scaled input variables, $\chi_{fuel}/10$ and χ_{vgt}. The scales are chosen based on range of values for each variable and relative importance in the control objectives. The dominance of the diagonal elements of the two-input two-output system at DC indicates, as expected, that χ_{fuel} strongly affects the steady-state value of N_e and χ_{vgt} strongly affects the steady-state value of ϕ.

The effects of χ_{fuel} on N_e and ϕ illustrate the severe tradeoff between fast engine speed tracking and tight air-to-fuel ratio control in a conventional fixed geometry turbocharged diesel engine. Specifically, the peak of the interaction between χ_{fuel} and ϕ occurs at 5 rad/sec and causes fast fuel commands to act as a disturbance to the ϕ subsystem. Therefore, to avoid undesirable disturbances of the air-to-fuel subsystem, the closed loop fuel command must be designed to roll off before the frequency of interaction resulting in slow torque response. The variable geometry turbocharger, on the other hand, has enough authority to reject the disturbances that χ_{fuel} imposes to ϕ without significantly affecting N_e. Hence, a two-input two-output feedback control design can potentially enhance fast engine speed transients without degrading emission performance.

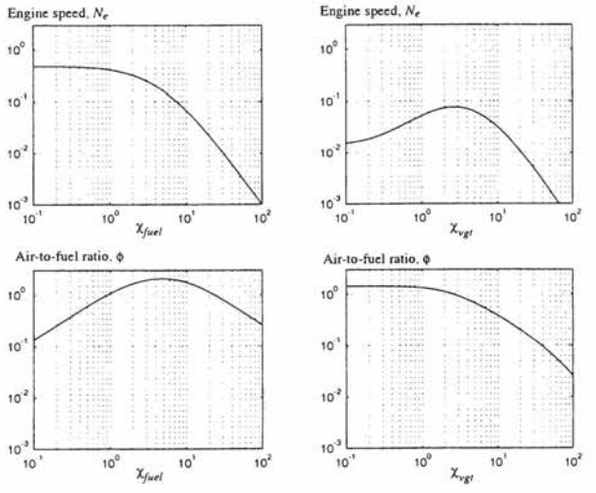

Figure 3: Bode magnitude plots of the input, χ_{fuel} and χ_{vgt}, to the output, N_e and ϕ at a nominal operating point.

We note here that regulation or disturbance rejection in engine speed can successfully be used to regulate ship speed or maintain constant heading in rough seas. This argument is based on the similarity of the two speeds, u and N_e. In particular, ship speed exhibits slightly slower dynamics than the engine speed. In addition, engine speed is one of the easily measured variables, in contrast to ship speed, which renders it more suitable for control design.

On the other hand, finding an appropriate measurement for the air-to-fuel ratio regulation is not straight forward [11]. An intake manifold pressure measurement is currently used for fuel limiting based on the steady-state estimation of combustion air and air-to-fuel ratio. Robust and accurate estimation of transient air-to-fuel ratio will be the next stage of this work.

6 Control Designs

Three control design strategies are compared on the above model. We assume that a measurement of the air-to-fuel ratio is available. This allows us to consider the VGT related control authority issues independently of any issues that would arise from the practical requirement of using only an estimate of the air-to-fuel ratio.

The first strategy uses a more standard proportional-integral (PI) design to control the engine speed, N_e, by actuating the fuel, χ_{fuel}. This has been tuned to give a good engine speed response to commanded engine speed step changes. Figure 4 illustrates the configuration. Note that this does not allow the air-to-fuel ratio to be set independently of the engine speed since the inlet guide vanes are held fixed at 0.38. This configuration does not require the measurement (or estimation) of the air-to-fuel ratio.

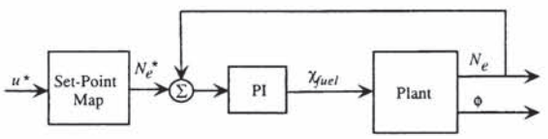

Figure 4: PI configuration for engine speed control

It is known—and will be evident in our simulations—that this configuration can produce undesirable transients in the air-to-fuel ratio. The standard approach to alleviating this problem uses a fuel limiter when the air-to-fuel ratio drops below a specified value. This configuration is illustrated in Figure 5. In our system the limiter adjusts the commanded fuel input to prevent the air-to-fuel ratio from dropping below $\phi = 24$. A measurement (or accurate estimation) of the air-to-fuel ratio is assumed. The PI controller now contains a standard antiwindup scheme to prevent the fuel limiter from causing controller saturation induced transients.

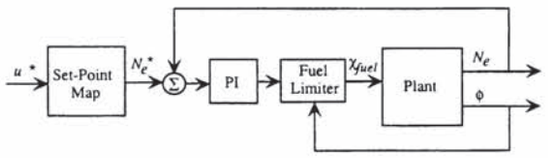

Figure 5: PI with fuel limiter configuration for engine speed and air-to-fuel ratio transient control

The design strategy for the variable geometry turbocharged engine (designated as MIMO in the subsequent analysis) uses measurements of both engine speed, N_e, and air-to-fuel ratio, ϕ, and is illustrated in Figure 6. This allows tracking of both engine speed, N_e^*, and air-to-fuel ratio, ϕ^*. A weighted linear quadratic Gaussian (LQG) design, based on the linearized model, has been tuned for both transient performance and integral type (zero steady state error) tracking of N_e^* and ϕ^*. The relative weighting between the regulated variables and the actuators is the same as that used in the Bode plots in Figure 3.

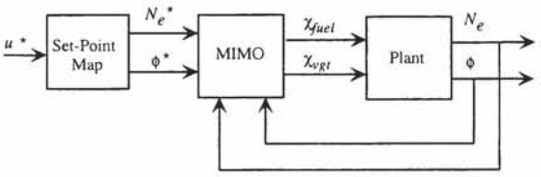

Figure 6: MIMO configuration for engine speed and air-to-fuel ratio control

7 Simulation Results

The above controllers have been evaluated on the nonlinear simulation model. The test maneuver involves a step change in ship speed from 18.6 knots to 21.2 knots. The set-point map generates a change in N_e^* from 1435 rpm to 1770 rpm, and a change in ϕ^* from 24.8 to 24.0. The closed-loop engine speed and air-to-fuel ratio responses are given in Figure 7. The corresponding actuation signals are shown in Figure 8.

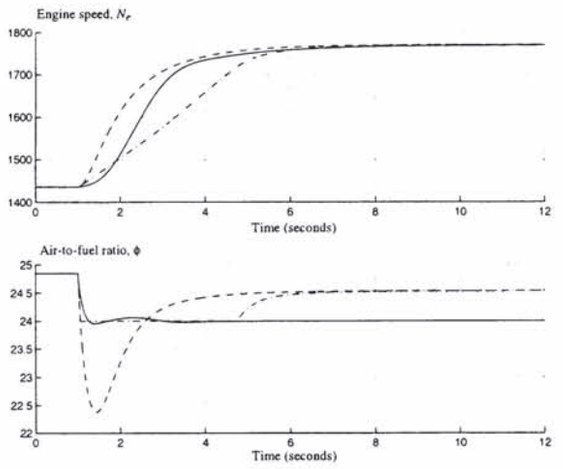

Figure 7: Closed-loop step responses: PI (dashed), PI with fuel limit (dot-dash), and MIMO (solid) control systems

The PI controller (dashed lines) gives the best engine speed response. This is achieved by a relatively fast

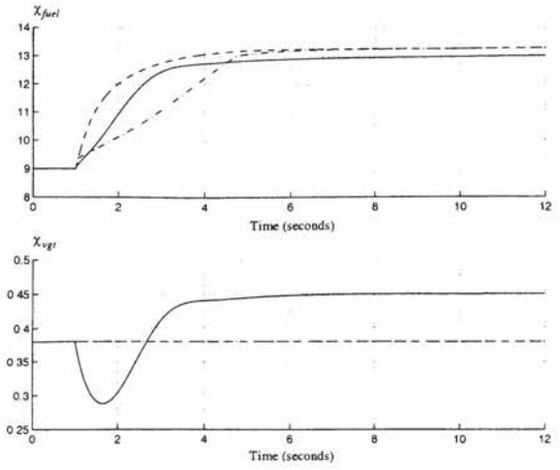

Figure 8: Closed-loop actuation signals: PI (dashed), PI with fuel limit (dot-dash), and MIMO (solid) control systems

change in fuel level which has the effect of producing a transient air-to-fuel ratio excursion which goes significantly below the excess smoke limit ($\psi = 24$).

As expected, the PI with fuel limiter (dot-dash lines) limits the rate of change of the fuel into the engine and prevents the air-to-fuel ratio from dropping below the smoke limit. However, it also has the effect of significantly degrading the engine speed response.

The MIMO controller (solid lines) gives an engine speed response which is close to that of the PI controller without creating a significant air-to-fuel ratio transient. This has been achieved by using the extra degree of freedom in the VGT actuation to control air-to-fuel ratio independently of the fuel flow rate. The VGT actuation is evident in Figure 8.

Note also that the MIMO controller uses the VGT actuator to provide a different steady state air-to-fuel ratio at the completion of the maneuver. The steady state value of ϕ has been chosen as discussed in Section 4 and results in the same engine speed with less fuel; hence giving more efficient steady-state operation.

8 Conclusions

The VGT gives an extra degree of freedom in the propulsion control system which allows some amount of independence between engine speed and air-to-fuel ratio. This gives significant performance advantages: in steady-state operation the air-to-fuel ratio can be tuned independently of engine speed to improve efficiency. In transient maneuvers the VGT can be used to prevent smoke producing transients in the air-to-fuel ratio without significantly degrading the engine speed response. Conventional approaches to this problem require a tradeoff between engine speed response and air-to-fuel ratio transient behavior. A MIMO controller must be used to take advantage of this additional capability.

References

[1] Haddad, S., and N. Watson, *Principles and Performance of Diesel Engineering,* Ellis Horwood, Chichester, 1984.

[2] J. B. Heywood, *Internal Combustion Engine Fundamentals,* McGraw-Hill, 1988.

[3] Kolmanovsky, I., Moraal, P., van Nieuwstadt, M., and Stefanopoulou, A., "Issues in modelling and control of intake flow in variable geometry turbocharged engines," *18th IFIP Conference on System Modelling and Optimization,* Detroit, July 1997.

[4] Lilly, L.R., *Diesel Engine Reference Book,* Butterworth, London, 1984.

[5] Moody, J.F., "Variable geometry turbocharging with electronic control," SAE paper No. 860107, 1986.

[6] Stefanopoulou, A., and I. Kolmanovsky, and J.S. Freudenberg, "Control of Variable Geometry Turbocharged Diesel Engine for Reduced Emissions," Proc. 1998 American Control Conference.

[7] Winterborne, D.E., and S. Jai-In (1991), "The application of modern control theory to a turbocharged diesel engine powerplant," , Proc. Instn. Mech. Engrs, Part I, Journal of Systems and Control Engineering, Vol. 205, pp. 69-83, IMechE, 1991.

[8] Watson N., and K. Banisoleiman (1988), "The Variable-Geometry Turbocharger Control System for High-output Diesel Engines," *SAE paper No. 880118,* 1988.

[9] Woodward, J.B., and R.G. Latorre (1984), "Modeling of Diesel Engine Transient Behavior in Marine Propulsion Analysis," SNAME Transaction, Vol 92, pp. 33-49.

[10] Valenti, M., "Luxury Liners Go Green," Mechanical Engineering, pp. 72-73, July, 1998.

[11] van Nieuwstadt, M., and I.V. Kolmanovsky, "Sensor Selection for EGR-VGT Control of a Diesel Engine," submitted International Conf. on Advances in Vehicle Control and Safety, 1998.